MAIN, P., HULL, S. E., LESSINGER, L., GERMAIN, G., DECLERCQ, J.-P. & WOOLFSON, M. M. (1978). *MULTAN78. A System of Computer Programs for the Automatic Solution of Crystal Structures from X-ray Diffaction Data*. Univs. of York, England, and Louvain, Belgium.

NORDMAN, C. E. & SCHMIDTKONS, D. L. (1965). *Acta Cryst.* **18**, 764–767.

SHELDRICK, G. M. (1976). *SHELX76*. Program for crystal structure determination. Univ. of Cambridge, England.

TIMMERMANS, J. (1961). *Phys. Chem. Solids*, **18**, 1–8.

Acta Cryst. (1991). B47, 789–797

Transferability of Deformation Densities among Related Molecules: Atomic Multipole Parameters from Perylene for Improved Estimation of Molecular Vibrations in Naphthalene and Anthracene

BY CAROLYN PRATT BROCK

Department of Chemistry, University of Kentucky, Lexington, KY, USA

JACK D. DUNITZ

Organic Chemistry Laboratory, ETH-Zentrum, Zurich, Switzerland

AND F. L. HIRSHFELD†

Department of Structural Chemistry, Weizmann Institute of Science, Rehovot, Israel

(*Received* 3 *October* 1990; *accepted* 2 *April* 1991)

Abstract

Earlier crystallographic refinements of naphthalene and anthracene against X-ray data recorded at five and six temperatures, respectively, have been repeated with atomic charge-deformation parameters transferred from a low-temperature study of perylene. Inclusion of these parameters causes the in-plane molecular translation amplitudes to decrease, and those normal to the plane to increase, with respect to values obtained with the spherical-atom model. The revised translation tensors are systematically smaller than those predicted by published lattice-dynamical calculations but the librations agree somewhat better. Their temperature dependence shows no anomalous behavior and accords qualitatively with the simplified model of Cruickshank [*Acta Cryst.* (1956), **9**, 1005–1009].

Introduction

In fitting a set of model parameters to experimental data, as in crystal structure refinement, it is often advantageous to reduce the flexibility of the model by fixing those parameters that are better known, from theory or previous experiments, than they can be determined from the observed data. Thus, for macromolecular structures yielding low-resolution X-ray data, it is routine to simplify the structural model by constraining bond lengths and angles or fixing the geometry of such groups as phenyl substituents. Even the use of atomic scattering factors calculated for spherical atoms constitutes such a simplification. This practice has the great advantage that the structure factors can be calculated by summation over the atoms, with a few parameters per atom, rather than by integration over the electron density. However, it is well known that the spherical-atom approximation may produce severe systematic errors in the refined atomic parameters (Ruysink & Vos, 1974; Hirshfeld, 1976). A powerful way to eliminate such errors is to refine electron deformation (multipole) parameters together with the atomic coordinates and displacement parameters (Stewart, 1976; Hansen & Coppens, 1978; Hirshfeld, 1991), but such a refinement requires highly accurate and extensive X-ray data. What if the data available are inadequate for such a treatment? One possibility is to set the deformation parameters at their most likely values, estimated either from theoretical electron density distributions or from multipole analyses of chemically related molecules.

The present study is an initial attempt in this direction. Its specific aim is to improve the temperature-dependent anisotropic displacement parameters (ADP's) of naphthalene between 92 and 239 K and of anthracene between 94 and 295 K that were derived by conventional least-squares analyses from X-ray data of moderate resolution (Brock &

† Deceased, 20 May 1991.

0108-7681/91/050789-09$03.00

Dunitz, 1982, 1990). For this purpose we have introduced atomic multipole parameters transferred from a study of perylene based on much more extensive diffraction data (Hirshfeld, Hope & Rabinovich, to be published – hereafter HHR). These data, recorded at 83 K and extending to a reciprocal radius H_{max} = 2·52 Å^{-1}, have led to a detailed map of the charge-deformation density of perylene. We hoped that, because of the close chemical relation of perylene to naphthalene and, less directly, to anthracene, the results of the perylene study might be used to model both their deformation densities.

Transferred deformation densities

Given the static deformation density of perylene, we can imagine several options for simulating a corresponding density for naphthalene. We could, for example, select the deformation density above the plane bisecting (approximately) the C(1)—C(10), C(3)—C(8), and C(5)—C(6) bonds of perylene (see Fig. 1 for atom numbering) and reflect it across this plane to complete a simulated molecule of naphthalene. Alternatively, we might divide the perylene deformation density into atomic fragments, for example *via* the stockholder partitioning recipe (Hirshfeld, 1977*a*; Eisenstein, 1988), assemble the fragments corresponding to half the perylene molecule, replacing those assigned to the tertiary carbon atoms C(7) and C(9) by reflected copies of the diatomic fragments C(4)—H(4) and C(2)—H(2), and finally average the deformation densities of C(1) and C(10), of C(3) and C(8), and of C(5) and C(6). Either of these procedures would produce a more or less acceptable model deformation density for naphthalene, but in a form that would not readily serve our particular purpose. We prefer that the deformation density be expressed as a sum of atomic terms amenable to analytic Fourier transformation, so as to provide modified non-spherical atomic scattering factors for use in our crystallographic refinements. The experimentally derived perylene deformation density (HHR) is in just such a form, having been obtained *via* the refinement program *LSEXP* (Hirshfeld, 1977*b*), which treats the static molecular deformation density as a sum of atom-centered fragments, each expanded in a basis of analytic functions $\rho_{i,k}(\mathbf{r})$ having the general form, expressed in local polar coordinates,

$$\rho_{i,k}(r,\theta_k) = r^n \exp(-\alpha_n r)\cos^n\theta_k. \qquad (1)$$

Our plan, therefore, was to extract such atom-centered fragments from the perylene study and use them to model the naphthalene and anthracene deformation densities, so permitting the refinement of these structures with the same *LSEXP* program.

A drawback of the atomic fragments from the *LSEXP* refinement is that they are poorly defined and less compactly localized than those provided by the stockholder recipe. In perylene they carry net charges ranging from −0·53 to +0·59 e, as against values between −0·09 and +0·08 e from the stockholder partitioning of the same deformation density. However, a slight modification of the perylene refinement permitted the derivation of reasonably transferable fragments for the construction of simulated deformation densities of the target molecules.

Although the perylene molecule occupies a general position in its crystal, HHR had imposed on their model deformation density the *mmm* symmetry of the free molecule. Thus, with regard to its static deformation density, the effective asymmetric unit comprised just one six-membered ring, in which atomic fragments C(1), C(2), C(9) and C(10) had local symmetry *m* (reflection in a local fit to the mean molecular plane) while atoms C(3) and C(8) had *mm* symmetry. All H atoms were assigned identical deformation densities with *mm* local symmetry. We adapted this model to our problem by imposing further constraints appropriate to the molecular symmetry of naphthalene and anthracene. Thus the deformation densities of atoms C(1) and C(10) and those of atoms C(3) and C(8) were each made identical in corresponding orientations. The perylene refinement was accordingly repeated with four, rather than six, independent types of carbon fragment plus one type of hydrogen. By reducing in this way the number of adjustable parameters, we hoped to remove some of the arbitrariness in the definition of the atomic fragments without unduly impairing their ability to model the deformation density of perylene.

One further change was required to assure that this refinement of the perylene deformation density would yield electrically neutral models of naphtha-

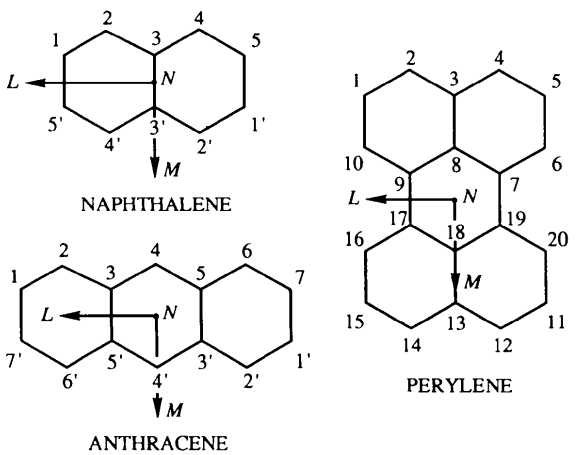

Fig. 1. Atomic numbering in naphthalene, anthracene and perylene.

lene and anthracene. For naphthalene the net charge of the C(9) fragment was constrained to equal the sum of the net charges of the C(2) and H fragments that would replace it in the formal conversion of half a molecule of perylene into a molecule of naphthalene. For anthracene, an analogous constraint was imposed, allowing for the further replication of the fragment C(2)—H, after symmetrization, in the 4 and 4′ positions of anthracene. Thus, two separate but similar refinements were performed against the perylene X-ray data to provide deformation parameters for transfer to the naphthalene and anthracene structures, respectively.

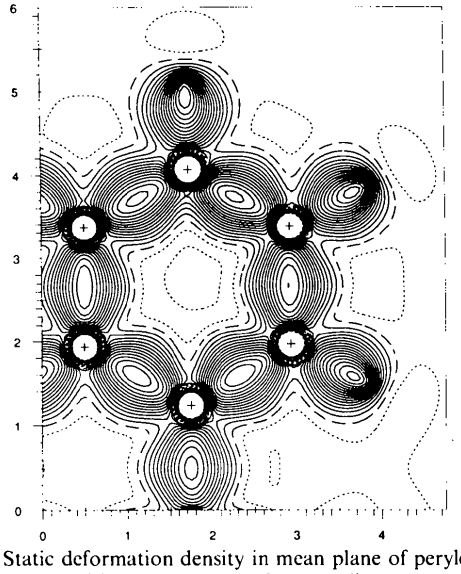

Fig. 2. Static deformation density in mean plane of perylene from refinement with symmetry and neutrality constraints for modeling naphthalene density. About one-quarter of the perylene molecule is shown. Contour interval 0·05 e Å $^{-3}$.

Table 1. *Net charges of atomic fragments from constrained refinements of perylene deformation density*

	Naphthalene model	Anthracene model
C(1) = C(10)	+0·489	+0·392
C(2)	−0·009	+0·035
C(3) = C(8)	−0·013	+0·187
C(9)	−0·246	−0·248
H	−0·237	−0·253

In these refinements only the deformation parameters were adjusted, all other parameters being fixed at the values obtained by HHR with their more flexible model. With only 95 variable parameters, as against 134 deformation parameters plus a scale factor and 216 atomic coordinates and displacement parameters refined by HHR, the weighted discrepancy factor $wR(F^2)$ rose from 0·0262 to 0·0274 in each case. This modest increase suggests that our additional constraints had, as hoped, simply eliminated some near-redundancy in the original model without severely compromising its flexibility. The resulting static deformation density for perylene (Fig. 2, from the naphthalene model; the anthracene model gave a virtually indistinguishable map) is very similar to that of HHR, differing from it most conspicuously in the symmetric appearance of the peaks in the C(1)—C(10) and C(3)—C(8) bonds. The slight asymmetry in these regions found by HHR, whether or not it is significant in perylene, is quite irrelevant for naphthalene and anthracene. The fragment charges from the new refinements (Table 1)

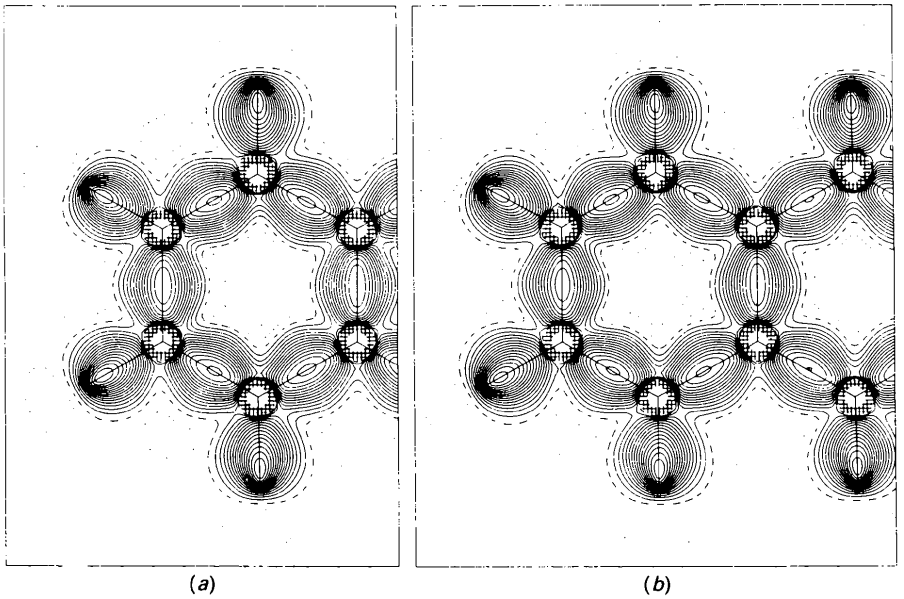

Fig. 3. Static deformation density in mean planes of naphthalene and anthracene transferred from perylene refinements. Contour interval 0·05 e Å $^{-3}$. (*a*) Naphthalene. (*b*) Anthracene.

were in the range −0·25 to +0·49 e for naphthalene, −0·25 to +0·39 e for anthracene.

Complete expansions of the transferred atomic fragments are given in Supplementary Tables *S*1 and *S*2.* Fig. 3 shows the deformation densities constructed from these fragments in the mean molecular planes of naphthalene and anthracene. While they do not represent the most accurate deformation densities that could be produced for these molecules, they surely provide a major improvement on the spherical-atom model and should allow the derivation of more reliable atomic displacement parameters than were obtained previously.

New naphthalene and anthracene refinements

The present set of refinements used all recorded reflections, up to $H_{max} = 1{\cdot}3$ Å $^{-1}$, including those with negative net intensities. An isotropic extinction correction increased the largest values of F_o by *ca* 3% for all data sets except the anthracene data at 295 K, where the largest correction approached 8%. (Extinction in the anthracene crystal decreased sharply on cooling from 295 to 259 K but showed no systematic variation with further cooling.) Refinement was on F^2, with variances (reciprocal weights) estimated as the sum of a Poisson term, for counting statistics, plus $(pF^2)^2$, with $p = 0{\cdot}03$ for naphthalene, 0·02 for anthracene.

In the earlier studies (Brock & Dunitz, 1982, 1990) the anisotropic displacement parameters U^{ij} of the carbon atoms were refined independently; after subtraction of calculated contributions from internal molecular vibrations, the adjusted ADP's were used for the derivation of molecular rigid-body translation and libration tensors **T** and **L** *via* the program *THM* (Trueblood, 1978). For the present study this procedure was reversed. In the *LSEXP* refinements, the internal-mode contributions to the ADP's of all atoms, including hydrogen, were added to the mean-square amplitudes derived from the variable molecular **T** and **L** tensors, whose components were refined directly, along with the atomic coordinates, against the diffraction data. This constraint on the ADP's reduced the number of independent parameters from 62 to 40 for the naphthalene refinement, from 84 to 49 for anthracene. Both methods assume the same separability of internal and lattice vibrations, which is probably valid for naphthalene and not too severe an approximation for anthracene, whose internal and external frequencies overlap slightly (Criado, 1989). In fact the two methods are nearly equivalent, provided the weight matrix for the rigid-body fit is based on the full covariance matrix of the ADP's, as derived from the unconstrained refinement (see Pawley, 1972). Otherwise, *e.g.* if the rigid-body program accepts only a diagonal weight matrix, constrained refinement is to be preferred as providing more reliable estimates of the molecular T^{ij} and L_{ij} components and of their standard deviations. On the other hand, this one-stage refinement of the molecular vibration parameters deprives us of the opportunity to examine the independent ADP's for evidence of any incompatibility with our vibration model. For both structures, however, the ADP's from the earlier studies (Brock & Dunitz, 1982, 1990) had already been shown to fit the rigid-body model, within their estimated accuracy, with or without correction for the internal vibrations.

Summary data on the new refinements for naphthalene and anthracene are presented in Tables 2 and 3, respectively. Atomic coordinates are listed in Supplementary Tables *S*3 and *S*4; bond lengths before and after correction for vibrational shortening are given in Tables *S*5 and *S*6.* The C—C distances have been corrected for rigid-body libration alone while the C—H corrections assume the motion of

Table 2. *Summary data on naphthalene refinements*

	92 K	109 K	143 K	184 K	239 K
No. of reflections	787	791	796	804	820
No. of $F_o^2 < 0$	20	14	15	29	34
No. of parameters	40	40	40	40	40
R, including $F_o^2 < 0$	0·027	0·028	0·026	0·027	0·029
R, excluding $F_o^2 < 0$	0·026	0·027	0·025	0·024	0·027
$wR(F^2)$	0·059	0·060	0·060	0·061	0·058
S	1·31	1·30	1·27	1·25	1·08
Max. Δ/σ	0·002	0·001	0·002	0·003	0·003

Table 3. *Summary data on anthracene refinements*

	94 K	140 K	181 K	220 K	259 K	295 K
No. of reflections	1045	1057	1063	1069	1075	1085
No. of $F_o^2 < 0$	125	132	134	167	182	161
No. of parameters	49	49	49	49	49	49
R, including $F_o^2 < 0$	0·062	0·067	0·072	0·086	0·099	0·080
R, excluding $F_o^2 < 0$	0·048	0·049	0·051	0·060	0·068	0·060
$wR(F^2)$	0·065	0·058	0·058	0·061	0·062	0·069
S	1·00	1·02	1·01	0·99	0·95	0·98
Max. Δ/σ	0·04	0·10	0·11	0·13	0·04	0·08

Table 4. *Average libration-corrected bond lengths* (Å)

Naphthalene		Anthracene	
C(1)—C(5′)	1·4214 (6)	C(1)—C(7′)	1·4313 (8)
C(1)—C(2)	1·3782 (4)	C(1)—C(2)	1·3691 (5)
C(2)—C(3)	1·4247 (3)	C(2)—C(3)	1·4339 (4)
C(3)—C(3′)	1·4263 (6)	C(3)—C(5′)	1·4407 (6)
		C(3)—C(4)	1·4026 (4)
C(1)—H(1)	1·104 (4)	C(1)—H(1)	1·129 (4)
C(2)—H(2)	1·117 (4)	C(2)—H(2)	1·113 (4)
		C(4)—H(4)	1·080 (6)

* Lists of structure factors, bond lengths, atomic coordinates and transferred atomic deformation densities have been deposited with the British Library Document Supply Centre as Supplementary Publication No. SUP 54089 (161 pp.). Copies may be obtained through The Technical Editor, International Union of Crystallography, 5 Abbey Square, Chester CH1 2HU, England.

* See deposition footnote.

Table 5. *Naphthalene molecular translation and libration tensors*

Temp. (K)	Referred to crystal axes a, b, c						Referred to molecular axes L, M, N					
	$T^{ij} \times 10^5$ (Å^2)			L_{ij} (deg^2)			$T^{ij} \times 10^5$ (Å^2)			L_{ij} (deg^2)		
92	615 (24)	21 (14)	569 (15)	7·74 (25)	0·13 (13)	−5·29 (34)	983 (18)	−131 (10)	184 (11)	5·68 (41)	0·87 (9)	−0·28 (14)
		776 (20)	4 (10)		4·46 (13)	−1·07 (15)		796 (20)	42 (12)		3·78 (13)	0·19 (8)
			1087 (18)			8·03 (59)			552 (27)			4·80 (11)
109	734 (24)	31 (14)	642 (15)	9·29 (26)	0·09 (13)	−6·11 (35)	1136 (18)	−143 (10)	179 (11)	6·27 (42)	1·03 (9)	−0·44 (15)
		881 (20)	11 (11)		5·06 (13)	1·14 (15)		915 (20)	32 (12)		4·31 (13)	0·12 (9)
			1238 (18)			8·92 (60)			659 (27)			5·79 (11)
143	985 (25)	41 (15)	770 (16)	12·23 (28)	0·03 (14)	−8·12 (37)	1547 (18)	−148 (11)	141 (11)	8·24 (45)	1·38 (10)	−0·67 (16)
		1173 (21)	11 (11)		6·66 (14)	−1·47 (16)		1204 (21)	47 (13)		5·61 (14)	0·23 (10)
			1591 (19)			11·71 (64)			919 (28)			7·64 (12)
184	1342 (26)	93 (16)	986 (17)	17·10 (32)	0·22 (16)	−11·51 (41)	2123 (19)	−166 (12)	119 (12)	12·02 (51)	1·87 (12)	−0·94 (18)
		1565 (22)	23 (13)		9·10 (15)	−2·16 (19)		1632 (22)	32 (14)		7·78 (15)	0·12 (11)
			2122 (19)			16·98 (71)			1240 (29)			10·55 (14)
239	1956 (26)	158 (17)	1428 (17)	23·88 (34)	0·26 (18)	−15·60 (44)	3109 (19)	240 (12)	165 (12)	16·91 (54)	2·54 (13)	−1·10 (20)
		2186 (21)	24 (13)		13·43 (17)	−2·87 (21)		2318 (22)	−3 (14)		11·64 (17)	0·18 (13)
			3106 (20)			23·63 (75)			1765 (29)			15·21 (15)

Table 6. *Anthracene molecular translation and libration tensors*

Temp. (K)	Referred to crystal axes a, b, c						Referred to molecular axes L, M, N					
	$T^{ij} \times 10^5$ (Å^2)			L_{ij} (deg^2)			$T^{ij} \times 10^5$ (Å^2)			L_{ij} (deg^2)		
94	483 (32)	37 (20)	258 (19)	3·4 (4)	0·3 (1)	−1·9 (6)	1059 (19)	7 (12)	−79 (13)	2·68 (67)	0·30 (10)	0·37 (18)
		526 (25)	−16 (14)		1·9 (1)	−0·6 (2)		542 (24)	−7 (17)		1·85 (10)	−0·21 (8)
			847 (20)			3·8 (10)			472 (36)			2·28 (10)
140	762 (31)	31 (20)	455 (19)	5·5 (4)	0·2 (1)	−3·4 (6)	1554 (18)	−4 (12)	54 (12)	5·25 (67)	0·36 (11)	0·90 (19)
		887 (24)	−34 (14)		3·0 (1)	−1·2 (2)		884 (24)	27 (17)		2·73 (11)	−0·27 (9)
			1308 (19)			7·4 (10)			763 (35)			3·94 (10)
181	1147 (31)	65 (20)	661 (19)	7·9 (4)	0·2 (1)	−4·9 (6)	2105 (19)	14 (12)	−83 (13)	6·34 (69)	0·48 (11)	0·49 (20)
		1282 (25)	−35 (14)		3·6 (1)	1·2 (2)		1300 (24)	8 (17)		3·39 (11)	0·49 (9)
			1790 (19)			9·1 (10)			1127 (36)			5·19 (11)
220	1470 (34)	40 (22)	942 (21)	9·7 (4)	0·2 (1)	−5·9 (6)	2646 (21)	−15 (13)	17 (14)	8·32 (75)	0·70 (13)	1·07 (23)
		1674 (27)	−77 (16)		4·8 (1)	−1·8 (2)		1664 (27)	46 (19)		4·33 (13)	−0·47 (11)
			2358 (21)			11·7 (11)			1454 (39)			6·80 (12)
259	1773 (37)	98 (24)	1139 (22)	12·0 (5)	0·5 (2)	−7·9 (7)	3323 (23)	38 (15)	0 (16)	11·51 (82)	0·82 (14)	1·46 (26)
		2093 (30)	51 (17)		6·0 (1)	−2·4 (2)		2108 (29)	58 (21)		5·57 (14)	−0·60 (13)
			2948 (23)			16·2 (12)			1732 (42)			8·12 (14)
295	2247 (42)	124 (28)	1445 (26)	14·3 (5)	0·7 (2)	8·9 (8)	4051 (27)	46 (17)	24 (18)	13·57 (92)	1·13 (16)	2·02 (30)
		2494 (35)	73 (20)		7·1 (2)	−3·2 (2)		2543 (34)	10 (25)		6·58 (16)	−0·93 (15)
			3636 (27)			18·9 (13)			2161 (48)			9·95 (16)

each hydrogen to comprise a combination of molecular libration plus a riding motion on its attached carbon. The average libration-corrected lengths of the chemically independent bonds are listed in Table 4. In computing these averages, the corrected bond lengths have been weighted by the inverse variances of the corresponding uncorrected distances (Tables *S5*, *S6*), but the standard deviations in Table 4 have been increased uniformly by 50% for naphthalene and 20% for anthracene, in accordance with the scatter of the corrected values. These e.s.d.'s take no account of systematic errors, such as those arising from any remaining deficiencies of the charge-density model. The largest changes with respect to the C—C bond lengths derived *via* the spherical-atom model (Brock & Dunitz, 1982, 1990) are an increase of 0·006 Å for the C(1)—C(5′) bond in naphthalene, and of 0·008 Å for the C(1)—C(2) bond in anthracene. The C—H distances, undoubtedly lengthened by anharmonic stretching vibrations, mostly exceed the expected equilibrium bond lengths.

Molecular vibration tensors

Tables 5 and 6 present the derived T^{ij} and L_{ij} parameters, referred both to the crystal axes and to the molecular inertial axes* (Fig. 1), for naphthalene at

* The molecular axes L, M, N follow the convention adopted by Cruickshank (1956*a*, 1957) and most subsequent authors, which places atom C(1) of each molecule at positive L, negative M (Fig. 1). This differs from the orientation chosen for naphthalene by Brock & Dunitz (1982), whose axes x_1 and x_2 have the opposite sense to our axes L and M, respectively. Thus the (13) and (23) cross terms in their inertial system are reversed in sign with respect to those given in our Table 5.

five and anthracene at six temperatures. Compared with the values obtained in the earlier studies, the diagonal components of the **T** and **L** tensors in the molecular axial system show appreciable systematic changes. In naphthalene, the in-plane translation components T^{11}(mol) and T^{22}(mol) decrease by about 0·001 Å^2, while the out-of-plane component T^{33}(mol) increases by nearly 0·002 Å^2, all these changes being fairly independent of temperature. All three diagonal libration components L_{ii}(mol) decrease at all temperatures, the largest decrease, amounting to 1–2 deg^2, being in the component L_{11}(mol) about the long molecular axis. The changes in anthracene are qualitatively similar but their magnitudes differ in a systematic manner. Here the in-plane translation components T^{11}(mol) and T^{22}(mol) decrease much more, by about 0·007 and 0·005 Å^2, respectively, while T^{33}(mol) increases by about 0·001 Å^2. The long-axis libration L_{11}(mol) mostly decreases by 0–2 deg^2 while L_{22}(mol) and L_{33}(mol) decrease more uniformly by about 0·5 deg^2. In both structures the decrease in the in-plane translation components and the increase in the out-of-plane component are many times the respective estimated standard deviations. These changes seem to offset the major effects of the deformation density near the carbon centers, which expands the atomic charge clouds towards the bonding regions while contrac-

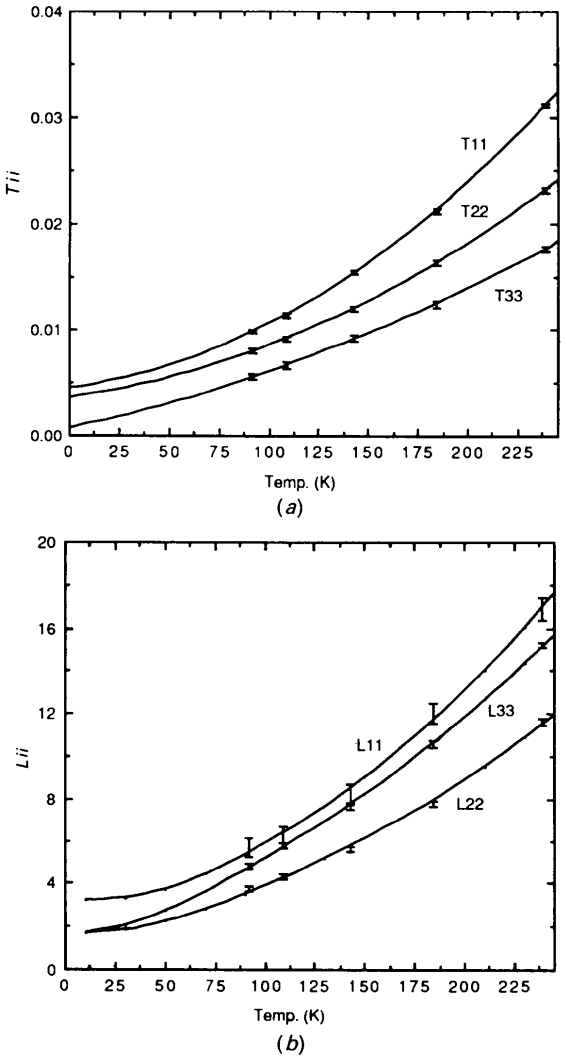

Fig. 4. Diagonal components, referred to molecular axes, of molecular **T** and **L** tensors of naphthalene at five temperatures. Error bars have length 2σ. (*a*) Translation components T^{ii} (Å^2). Smooth curves show quadratic fits to experimental points. (*b*) Libration components L_{ii} (deg^2). Smooth curves from equations (2) and (3).

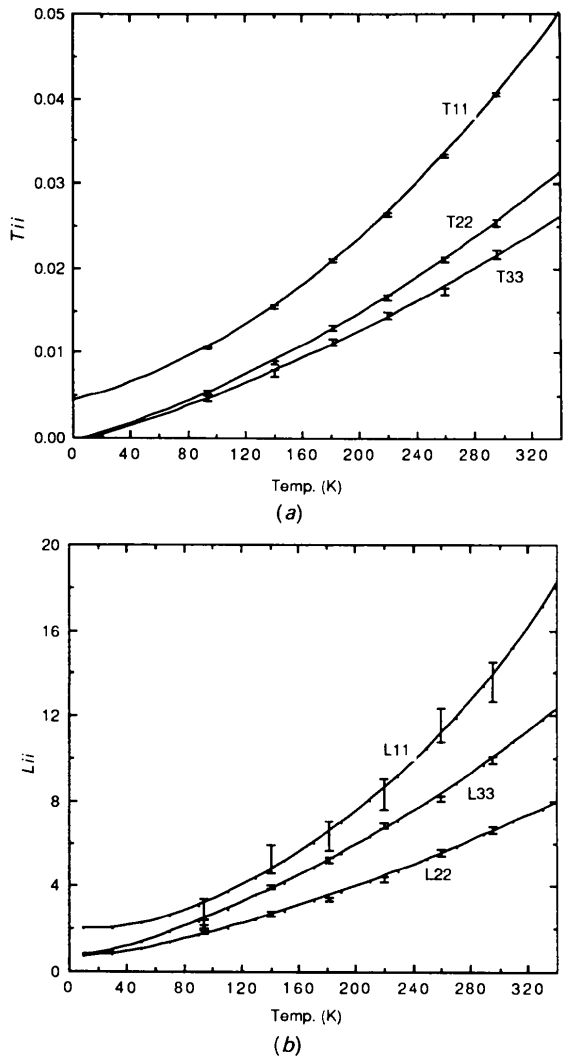

Fig. 5. Diagonal components, referred to molecular axes, of molecular **T** and **L** tensors of anthracene at six temperatures. Error bars have length 2σ. (*a*) Translation components T^{ii} (Å^2). Smooth curves show quadratic fits to experimental points. (*b*) Libration components L_{ii} (deg^2). Smooth curves from equations (2) and (3).

ting them in the out-of-plane direction. The changes in the libration components are less significant, relative to their estimated standard deviations, but are still largely systematic.

The temperature dependence of the T^{ii}(mol) and L_{ii}(mol) components is plotted in Figs. 4 and 5. For ease of comparison, the range of each of these plots extends from 0 to 0·69 times the corresponding melting temperature T_m. At corresponding reduced temperatures T/T_m, anthracene has appreciably larger translation amplitudes but mainly smaller librations than naphthalene. Each vibration component is seen to increase smoothly with temperature, with a scatter that is consistent with its estimated standard deviations (Tables 5, 6). The libration L_{11}(mol) of anthracene about its long molecular axis, which had earlier appeared to behave somewhat irregularly (Brock & Dunitz, 1990), still shows the largest deviations from a smooth temperature variation, but these are no greater than would be expected from its relatively poor experimental precision.

Comparison with lattice dynamics

Lattice-dynamical calculations for naphthalene and anthracene, and their perdeuterated analogs, have been reported by several authors (*e.g.* Pawley, 1967; Filippini, Gramaciolli, Simonetta & Suffritti, 1973; Bokhenkov, Rodina, Sheka & Natkaniec, 1978; Vovelle, Chedin & Dumas, 1978; Natkaniec *et al.*, 1980; Dorner *et al.*, 1982). Among the calculated vibration tensors pertinent to the temperature ranges covered by our experimental studies are the results on anthracene by Pawley (1967) at 300 K and by Vovelle *et al.* (1978), by Gramaccioli & Filippini (1983), and by Criado (1989) at 290 K, as well as the latter's results for naphthalene at 92 K. Also, Vovelle *et al.* (1978) have plotted the calculated temperature dependence of $L_{ii}(\text{mol})^{1/2}$ in naphthalene and listed both $T^{ii}(\text{mol})^{1/2}$ and $L_{ii}(\text{mol})^{1/2}$ for anthracene at 95 and 290 K. Their results agree remarkably well with the experimental curves in Figs. 4(*b*) and 5(*b*) except for the long-axis libration L_{11} in anthracene, which they calculate well above our experimental curve.

For an overall comparison of the calculated and observed vibration amplitudes, Table 7 lists the traces of the molecular **T** and **L** tensors from these several calculations together with the values, at the same or nearby temperatures, from our X-ray studies. The X-ray results yield much smaller values of Tr(**T**) than any of the calculations; the agreement for Tr(**L**) is somewhat better. The disagreement in the mean-square translation amplitudes may be partly attributed to our failure to correct for thermal diffuse scattering, which causes a systematic underestimation of the crystallographically determined

Table 7. *Traces of the molecular tensors* **T** *and* **L** *from lattice-dynamical calculations and X-ray diffraction*

	Naphthalene, 92 K		Anthracene, 290–300 K	
	Tr(**T**) (Å^2)	Tr(**L**) (deg^2)	Tr(**T**) (Å^2)	Tr(**L**) (deg^2)
Pa[a]			0·1016	30·1*
VCD[b]			0·1186	36·9*
GF[c] (rigid molecule)			0·1261	35·5
GF (non-rigid)			0·1332	36·8*
Cr[d] (without charges)	0·0334	15·8	0·1566	41·7
Cr (with charges)	0·0322	14·8	0·1427	37·1
BD[e]	0·0252	16·1	0·0973	32·8
Present study	0·0233	14·2	0·0875	30·1

References: (*a*) Pawley (1967); (*b*) Vovelle *et al.* (1978); (*c*) Gramaccioli & Filippini (1983); (*d*) Criado (1989); (*e*) Brock & Dunitz (1982, 1990).

* The calculated libration components, referred to molecular axes, are (in deg^2):

Pa	15·1	1·1	2·8	VCD	18·9	0·7	2·7	GF	17·9	3·4	−0·8
		6·0	0·5			6·8	0·2			8·4	−1·4
			9·0				11·2				10·4

atomic vibration amplitudes (Harada & Sakata, 1974). However, this unlikely to account for the total discrepancy, especially at 92 K.

Whatever the cause of the large and systematic disagreement in the translation amplitudes, it seems to affect the libration tensors much less. Table 7 presents the libration components from several of the lattice-dynamical calculations on anthracene, referred to the molecular axes, for direct comparison with our X-ray results at 295 K (Table 6). [In transforming the components reported by Gramaccioli & Filippini (1983) to the molecular coordinate system, we have used the rotation matrix derived from our experimental structure at 295 K.] The only major disagreement between the calculated and experimental tensor components concerns, again, the libration about the long molecular axis. Quantitatively, our experimental **L** tensor agrees best with the older calculations of Pawley (1967). These were based on the atom–atom potentials of Kitaigorodsky (1966), while the later studies used potential set IV of Williams (1967).

A similar comparison with the libration components reported by Criado (1989), for both structures, is hampered by the difficulty in identifying the coordinate axes to which these components are referred.

For a molecule librating in a harmonic potential with effective frequency ν_i about each of its inertial axes, the mean-square libration amplitudes, in radians^2, are

$$L_{ii}(\text{mol}) = (h/8\pi^2 I_i \nu_i)\coth(h\nu_i/2kT), \qquad (2)$$

where I_i is the inertial moment about axis i. This is the form taken by equation (5) of Cruickshank (1956*b*) with equal frequencies for the in-phase and

Table 8. *Intercepts* $\nu_i(0)$ (cm^{-1}) *and slopes* a_i (K^{-1}) *of libration frequencies* $\nu_i(T)$, *and their correlation coefficients* r, *from least-squares fit to observed mean-square amplitudes* L_{ii}(*mol*) *via* (2) *and* (3), *compared with corresponding parameters estimated from Raman frequencies* (*Suzuki et al.*, 1968) *at* 77 *and* 293 K

		From L_{ii} (mol)			From Raman frequencies	
	Axis i	$\nu_i(0)$	a_i	r	$\nu_i(0)$	a_i
Naphthalene	1	106·2 (41)	0·00094 (16)	0·952	136	0·00047
	2	79·3 (14)	0·00088 (7)	0·951	90	0·00067
	3	56·2 (6)	0·00075 (5)	0·950	66	0·00090
Anthracene	1	119·1 (99)	0·00101 (24)	0·965	139	0·00039
	2	66·2 (18)	0·00053 (9)	0·964	78	0·00044
	3	50·3 (9)	0·00063 (6)	0·963	55	0·00079

out-of-phase librations of the two molecules in the unit cell about each axis. Given the observed L_{ii}(mol) at any temperature T, we can solve for the effective frequency ν_i. The frequencies so calculated decrease almost linearly with increasing temperature, as envisioned by Cruickshank (1956*b*). In fact the smooth curves in Figs. 4(*b*) and 5(*b*) have been evaluated *via* (2), with each ν_i fitted to the linear expression

$$\nu_i(T) = \nu_i(0)(1 - a_i T), \qquad (3)$$

whose parameters $\nu_i(0)$ and a_i are listed, with their estimated standard deviations and correlation coefficient, in Table 8. The quality of the fits may be gauged from the overall goodness-of-fit S for each structure, defined by

$$S^2 = \sum_{i,T}[\Delta L_{ii}(T)]^2/(n - p).$$

For naphthalene (with $n = 15$ observations fitted by $p = 6$ parameters) $S = 1{\cdot}05$; for anthracene ($n = 18$, $p = 6$) $S = 1{\cdot}09$. The fitted frequencies are, however, systematically lower by up to 30% than the Raman frequencies cited by Cruickshank or than the more extensive frequency data of Suzuki, Yokoyama & Ito (1968) (Table 8). Correcting our diffraction data for thermal diffuse scattering would likely increase this discrepancy. The probable explanation, as demonstrated by Pawley (1967) and by Vovelle *et al.* (1978), lies in the appreciable dispersion of the lattice frequencies with varying wavevector **k**. The major contributions to the mean-square libration amplitudes L_{ii} come from regions of the Brillouin zone with frequencies ν_i much lower than those observed at $\mathbf{k} = 0$. This conclusion is supported by the lattice-dynamical calculations of Gramaccioli & Filippini (1983) and of Criado (1989). Substituting, for example, the a_g and b_g (in-phase and out-of-phase libration) frequencies at $\mathbf{k} = 0$ for non-rigid anthracene at 290 K from the former authors' Supplementary Table 2(*a*) into Cruickshank's equation (5), we obtain a value for Tr(**L**) of 20·9 deg^2, as compared with their calculated value of 36·8 deg^2 (Table 7). Nevertheless, the Cruickshank approximation serves very well for predicting the variation of the mean-square libration amplitudes with temperature, as indicated by the fit of the experimental L_{ii}(mol) to the smooth curves in Figs. 4(*b*) and 5(*b*) and by the qualitative agreement of the temperature dependence of the corresponding libration frequencies with that of the Raman frequencies measured by Suzuki *et al.* (1968).

Concluding remarks

A method has been devised for transferring experimentally derived deformation densities between chemically related molecules so as to avoid much of the systematic error in structural parameters arising from the use of the spherical-atom model in crystallographic refinements. The method may prove applicable to other situations where the X-ray data are not adequate, in accuracy and resolution, to permit a reliable deformation-density refinement.

Introduction of such simulated deformation densities produces systematic changes in the atomic displacement parameters that tend to oppose the effect of the deformation density near the atomic centers.

The revised displacement parameters in anthracene show no significant evidence for an anomalous temperature variation in the libration amplitude about the long molecular axis.

The experimentally derived molecular translation amplitudes are systematically smaller than those predicted by lattice-dynamical calculations, to a degree that probably cannot be fully explained by the effect of thermal diffuse scattering. The libration amplitudes show appreciably better agreement with the calculations.

The approximation of Cruickshank (1956*b*), if combined with the spectroscopically observable lattice frequencies, severely underestimates the libration amplitudes. However, it predicts quite well their approximate temperature dependence.

Whether our use of transferred deformation densities has actually led to *improved* values of the atomic ADP's cannot be answered with complete confidence at present as there are other sources of error whose effects cannot be quantitatively assessed. We do not know the true values of the ADP's and the lattice-dynamical values may not be too reliable a guide.

We are grateful for the patient and expert assistance of Dr Bernd Schweizer in overcoming countless computational problems. The Bitnet/Earnet electronic network was an indispensisble partner in our tricontinental collaboration. Financial support was generously provided by the Swiss National Science Foundation.

References

BOKHENKOV, E. L., RODINA, E. M., SHEKA, E. F. & NATKANIEC, I. (1978). *Phys. Status Solidi*, **85**, 331–342.
BROCK, C. P. & DUNITZ, J. D. (1982). *Acta Cryst.* B**38**, 2218–2228.
BROCK, C. P. & DUNITZ, J. D. (1990). *Acta Cryst.* B**46**, 795–806.
CRIADO, A. (1989). *Acta Cryst.* A**45**, 409–415.
CRUICKSHANK, D. W. J. (1956*a*). *Acta Cryst.* **9**, 915–923.
CRUICKSHANK, D. W. J. (1956*b*). *Acta Cryst.* **9**, 1005 1009.
CRUICKSHANK, D. W. J. (1957). *Acta Cryst.* **10**, 504–508.
DORNER, B., BOKHENKOV, E. L., CHAPLOT, S. L., KALUS, J., NATKANIEC, I., PAWLEY, G. S., SCHMELZER, U. & SHEKA, E. F. (1982). *J. Phys. C*, **15**, 2353–2365.
EISENSTEIN, M. (1988). *Int. J. Quantum Chem.* **33**, 127 158.
FILIPPINI, G., GRAMACCIOLI, C. M., SIMONETTA, M. & SUFFRITTI, G. B. (1973). *J. Chem. Phys.* **59**, 5088 5101.
GRAMACCIOLI, C. M. & FILIPPINI, G. (1983). *Acta Cryst.* A**39**, 784 791.
HANSEN, N. K. & COPPENS, P. (1978). *Acta Cryst.* A**34**, 909–921.
HARADA, J. & SAKATA, M. (1974). *Acta Cryst.* A**30**, 77–82.
HIRSHFELD, F. L. (1976). *Acta Cryst.* A**32**, 239–244.
HIRSHFELD, F. L. (1977*a*). *Theor. Chim. Acta*, **44**, 129–138.
HIRSHFELD, F. L. (1977*b*). *Isr. J. Chem.* **16**, 226–229.
HIRSHFELD, F. L. (1991). *Crystallogr. Rev.* In the press.
KITAIGORODSKY, A. (1966). *J. Chim. Phys.* **63**, 6–14.
NATKANIEC, I., BOKHENKOV, E. L., DORNER, B., KALUS, J., MACKENZIE, G. A., PAWLEY, G. S., SCHMELZER, U. & SHEKA, E. F. (1980). *J. Phys. C*, **13**, 4265–4283.
PAWLEY, G. S. (1967). *Phys. Status Solidi*, **20**, 347–360.
PAWLEY, G. S. (1972). *Advances in Structure Research by Diffraction Methods*, Vol. 4, edited by W. HOPPE & R. MASON, pp. 1–64. Oxford: Pergamon Press.
RUYSINK, A. F. J. & VOS, A. (1974). *Acta Cryst.* A**30**, 503–506.
STEWART, R. F. W. (1976). *Acta Cryst.* A**32**, 565–574.
SUZUKI, M., YOKOYAMA, T. & ITO, M. (1968). *Spectrochim. Acta Part A*, **24**, 1091–1107.
TRUEBLOOD, K. N. (1978). *Acta Cryst.* A**34**, 950–954.
VOVELLE, F., CHEDIN, M. P. & DUMAS, G. G. (1978). *Mol. Cryst. Liq. Cryst.* **48**, 261–271.
WILLIAMS, D. E. (1967). *J. Chem. Phys.* **47**, 4680–4684.

Acta Cryst. (1991). B**47**, 797–806

High-Pressure Phases of Cyclohexane-d_{12}*

BY N. B. WILDING, P. D. HATTON† AND G. S. PAWLEY

Department of Physics, University of Edinburgh, Mayfield Road, Edinburgh EH9 3JZ, Scotland

(*Received* 3 *September* 1990; *accepted* 15 *April* 1991)

Abstract

A neutron powder diffraction study has been performed to investigate the high-pressure phases of deuterated cyclohexane. The unit cell and space group of the previously unsolved high-pressure phases III and IV have been determined with the aid of *KOHL* – a version of Kohlbeck & Hörl's *TMO* indexing program [*J. Appl. Cryst.* (1978), **11**, 60–61]. At 5 kbar, 280 K, we find that phase III is orthorhombic with unit-cell parameters $a = 6{\cdot}587\ (3)$, $b = 7{\cdot}844\ (7)$, $c = 5{\cdot}295\ (3)$ Å, $Z = 2$, space group $Pmnn$, $R_I = 4{\cdot}2$, $R_{wp} = 8{\cdot}4\%$. Approximate molecular orientations have also been determined for phase III using a combination of lattice-energy minimization techniques and constrained Rietveld refinement. On decreasing the temperature at 5 kbar, a structural phase transition was observed at 265 K to phase IV, a monoclinic structure with unit-cell parameters $a = 6{\cdot}526\ (4)$, $b = 7{\cdot}597\ (6)$, $c = 5{\cdot}463\ (5)$ Å, $\beta = 97{\cdot}108\ (4)^\circ$ at 250 K, $Z = 2$, space group $P12_1/n1$. This phase, which was observed down to 175 K, is closely related to the orthorhombic phase III but differs greatly from the monoclinic phase II which exists under atmospheric pressure at temperatures below 186·1 K. A further phase transition between phases IV and II was found at 2 kbar, 175 K.

1. Introduction and background

It is a feature of many organic molecular crystals that they exhibit a rich variety of phase structure, both as a function of temperature and pressure. Although the adoption by a molecular crystal of a range of different structures is thought to owe much to the rules of compact packing, this is by no means the sole criterion and further influencing factors such as the directionality of bonding may also play a role (Kitaigorodski, 1971). The lack of a thorough understanding of the processes governing the formation of any given phase means that as yet, it is not possible to predict, *a priori*, which structure a given molecular crystal will adopt for prescribed values of the temperature and pressure. A clear elucidation for a simple molecular system of the adopted structures, together with the conditions under which they are formed is therefore a vital step towards the understanding of the mechanisms governing structural polymorphism. To this end we have chosen to investigate the high-pressure phases of cyclohexane which, whilst being a relatively simple and compact molecule, is also known to exhibit a wealth of phase structure.

* Neutron powder diffraction measurements were carried out at the Institut Laue–Langevin, Grenoble.

† Author to whom correspondence should be addressed.

0108-7681/91/050797-10$03.00